ORIGINAL ARTICLE

lajss.org Latin American Journal of Solids and Structures

www.lajss.org

On mathematical modeling of an orchard tower sprayer Dynamics excited by rheological magnetic damping

Rodrigo do Nascimento e Silva[a]*, José Manoel Balthazar[a,b], Mauricio Aparecido Ribeiro[a], Ângelo M. Tusset[a] and Jorge Luiz Palácios Félix[c]

[a]Department of Production Engineering, Federal University of Technology—Parana, Ponta Grossa 84017-220, Parana, Brazil. Email: rodrigo.1984@alunos.utfpr.edu.br, balthazar@utfpr.edu.br, mau.ap.ribeiro@gmail.com, tusset@utfpr.edu.br.

[b]Faculty of Mechanical Engineering, São Paulo State University, Bauru 17033-360, São Paulo, Brazil. Email: balthazar@utfpr.edu.br

[c]Department of Environmental Engineering and Sanitary, Federal University of the Southern Border. Cerro Largo, São Pedro 89802-112, Rio Grande do Sul, Brazil. Email: jorge.felix@uffs.edu.br

*Corresponding author

https://doi.org/10.1590/1679-78258151

Abstract

Tower sprayers play a vital role in agriculture, being designed to apply pesticides and fertilizers effectively. The dynamics of this equipment, especially the vibration of the tower, play a crucial role in the success of agricultural operations. Analyzing and understanding this vibration is critical to ensuring application accuracy while minimizing variations in chemical distribution. This understanding directly contributes to uniform plant coverage, improving spraying efficiency and reducing input losses. In addition, practical vibration analysis extends the life of tower components, optimizes operational safety, and promotes energy efficiency by reducing fuel consumption. Tower stability becomes crucial to prevent spills and ensure efficient use of available resources. In short, dynamics and vibration analysis in tower sprayers are critical elements for the precise, efficient, and safe application of agricultural inputs. This approach promotes sustainable practices and contributes significantly to the success of farming operations. As a result of this study, a 23.68% reduction in trailer vibration amplitude was achieved.

Keywords

Tower sprayers; vibration; dynamics; application precision; agricultural efficiency

Graphical Abstract

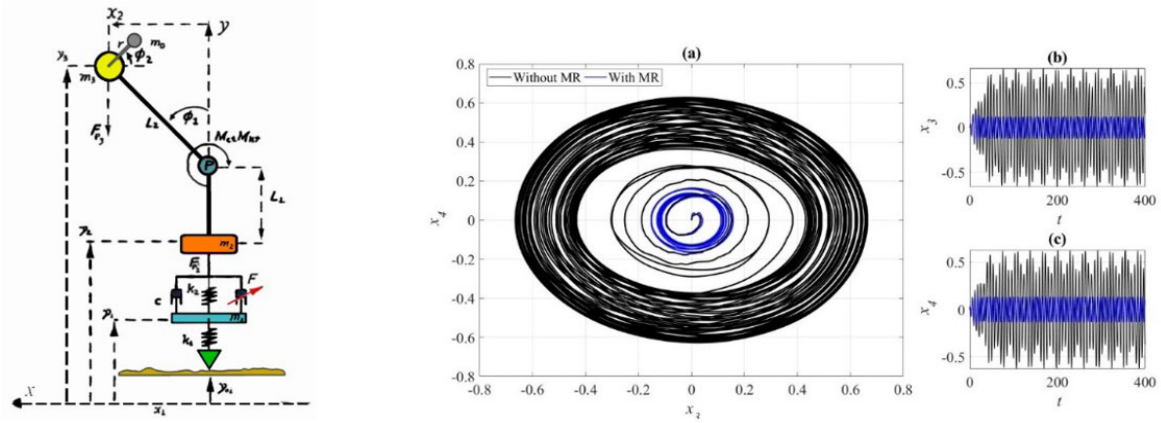

Received April 10, 2024. In revised form July 11, 2024. Accepted July 19, 2024. Available online July 22, 2024.
https://doi.org/10.1590/1679-78258151

Latin American Journal of Solids and Structures. ISSN 1679-7825. Copyright © 2024. This is an Open Access article distributed under the terms of the Creative Commons Attribution License, which permits unrestricted use, distribution, and reproduction in any medium, provided the original work is properly cited.

1 INTRODUCTION

Vibration reduction and dynamic analysis in tower sprayers in contemporary agriculture are fundamental to improving operational efficiency and ensuring the precise application of agricultural inputs. Minimizing vibration plays a crucial role in ensuring the precision of the spraying process, avoiding variations in the distribution of pesticides and fertilizers that could compromise the effectiveness of the treatment on the plants. In the studies listed below, we can see the concern to optimize the application of chemical products in orchards.

The research in (Garcerá et. al, 2017) revealed that only 45% of the pesticides applied to Mediterranean citrus plantations reached the target trees, representing an environmental risk for nearby areas. This highlights the need to improve spraying efficiency through new technologies and sprayer designs, considering climatic conditions and the stage of fruit growth. The data can be used to create a system for classifying spraying technologies based on their environmental impact, facilitating the authorization of pesticides.

This study (Ma et al., 2021) presents the development of a jet-controlled remote sprayer to solve the problems of low air supply and poor target accuracy in orchards. This tool is more suitable for crops in mountainous areas and improves the uniformity of pesticide application, which can be applied to adjacent fields. This study provides essential information on jet spraying operation and automatic spraying design.

According to (Ozkan, 2022), the choice of suitable equipment is crucial for effectively applying pesticides in vineyards and orchards due to variations in canopy structure and plantation characteristics. The main factors to consider when selecting a sprayer are its ability to deliver the required application rate, spray droplets of the appropriate size uniformly on the target and minimize spray losses to the ground and air.

On the other hand, assessing spray drift in the air (Arvidsson et al., 2014) is a challenge that requires the improvement of methods to ensure reliable spray mass balances. It is essential to employ well-documented and validated methods for all spray fractions, including airborne drift. In addition, the height of the sampling masts is crucial, with a minimum height of 4m being required in weed crops and 6m in crops treated with orchard sprayers to accurately quantify the airborne drift fraction.

The Orchard Sprayer Evaluation Process (Dekeyser et al., 2013) using laboratory experiments and computational fluid dynamics modeling is a reality, where the CFD simulation model used was developed to predict the exit velocity profile of the three sprayers at different distances from their exit and the vertical distribution of the spray along the height of a standardizer wall. The study of orchard sprayer evaluation has important implications for agriculture. It provides valuable information on the factors that influence the performance of this equipment, such as airflow patterns and the architecture of the air discharge unit. This information can be applied to improve the performance of sprayers, optimizing the efficiency of pesticide application in orchards. By enhancing this efficiency, sprayers can maximize the amount of pesticide needed to achieve the desired pest control, thus reducing the environmental impact of pesticide use in agriculture(Miranda-Fuentes et al., 2015).

According to (Kasner et al., 2020), the results of spray tests comparing old and new spraying technologies showed that air blast tower sprayers, specifically the directed air tower (DAT) and the multi-ventilator tower (MFT), showed reduced drift levels compared to the conventional axial air blast sprayer (AFA). The MFT significantly reduced drift levels by 35%, while the TAD showed a 7% reduction without statistical significance. These results suggest that tower sprayers are promising for reducing drift levels in modern orchards. For example, Figure 1 illustrates two fans.

Uniform spray coverage (Xun et al., 2022) is crucial to achieving effective pest and disease control in citrus groves. According to the study by (van Zyl et al., 2014), the use of organosilicon adjuvants, such as Break-Thru S240 and Break-Thru Union, can improve spray penetration into the citrus canopy, resulting in better coverage and penetration of pesticides, which in turn enhances pest and disease control.

The search for more sustainable and efficient agricultural practices has driven innovation in this sector, with ongoing efforts to improve application precision, reduce waste, and minimize environmental impact. It is recommended to consult specialized sources and manufacturers for more detailed information on this agricultural equipment's current scenario and future trends (Jacto S/A., 2024a).

This investigation by (McCoy et al., 2023) revealed important information about the use and calibration of canopy sprinklers in the PNW region. Despite the small sample size, this data can help grape growers select more appropriate spraying options and improve spraying practices. They understand sprinklers' basic form and function of sprinklers to minimize malfunction and maximize efficiency. Optimizing the use of pesticides through spraying is essential for crop efficiency and economy. The agricultural workforce must understand how sprinklers work, and agricultural extension can help fill the knowledge gap. It is necessary to update knowledge about the different models and techniques for spraying vineyards.

The study (Kira et al., 2018) highlights the effectiveness of the OP-FTIR technique for measuring spray drift and comparing the performance of agricultural sprayers. It emphasizes the importance of additional measures to better characterize spray drift, including longer distances and different types of sprays. Furthermore, it suggests that the

implementation of real-time tools to estimate droplet size distribution or the development of inverse modeling methods could enhance the use of the OP-FTIR technique.

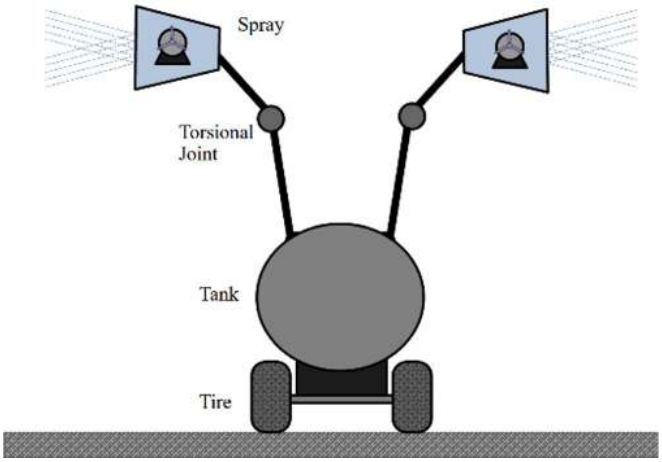

Figure 1: Simplified tower sprayer structure.

The results found by (Li et al., 2022), are based on years of research dedicated to improving spray performance on the abaxial side of leaves in orchards, by adjusting application parameters and improving the spray system. However, more research is still needed to fully understand the correlations between airflow speed and direction and the distribution of spray deposits. In addition, the dynamic behavior of droplets and leaves in the airflow will be further investigated to improve the understanding of air-assisted spraying. In short, the conclusion indicates the importance of adapting spraying methods according to the specific characteristics of fruit orchards to obtain an effective distribution of pesticides and optimize crop protection.

This research focused on spray drift in poplar plantations using pneumatic sprayers. It found that drift is lower in mature plantations than in young plantations due to the lower density of the canopy and the greater spacing between trees. It is recommended to use a spraying system that activates the spray nozzle only when necessary to minimize drift. The study emphasizes the importance of developing specific reference curves for poplar cultivation at different growth stages.

It presents research projects on developing variable air assist (VAA) systems for conventional fruit spraying. The VAA system can control the amount of air immediately and continuously and includes a spraying system on both sides of the sprayer. VAA with a double axial fan system produces high air volumes (20,000 m^3/hour) and low energy consumption (10 kW), suitable for fruit of specific sizes. It was concluded that the VAA is a valid example for future variable dose technologies and intelligent spraying for fruit. This article describes an innovative solution for agricultural sprays used in gardens to reduce application losses and save energy (Hołownicki et al., 2017).

According to (Grella et al., 2017), the ISO22866:2005 protocol helps determine spray pressure values in natural conditions, but it is challenging to simulate the flow problem of different spray configurations. Small changes in wind direction can impact ground spraying, while higher wind speeds can cause the aircraft to drift even more. Therefore, the ISO22866 protocol may not be suitable for comparing the risk assessment between different spray configurations.

Author (Patil et al., 2023) highlights the importance of reducing pesticide use and environmental pollution in orchards, suggesting the use of variable-rate spray treatments. This approach allows pesticides to be applied only where necessary, in a more economical and environmentally friendly way. The introduction of automatic sprayers, with adjustments based on the size and shape of orchards, is highlighted as a promising solution, with the application of technologies such as Artificial Intelligence and Machine Learning. The study aims to increase spraying efficiency by reducing soil losses and off-target drift. In short, exploring variable rate spraying techniques in orchards could reduce the excessive use of pesticides, with environmental and economic benefits.

In (Grella et al., 2017), the authors make a detailed analysis of the dynamics of the tower sprayer, which is an essential component in understanding its behavior during operation. This not only contributes to identifying potential structural failure points but also guarantees the integrity of the equipment, promoting excellent durability and operational safety.

Reducing vibration improves application efficiency, minimizes input waste, and plays a significant role in environmental sustainability. Optimizing the use of chemical products contributes to more responsible farming practices in line with the growing demands for sustainable agriculture. In addition, reducing vibration positively impacts operator comfort, creating a safer and more pleasant working environment. This holistic approach to optimizing dynamics in tower sprayers reflects the search for efficient, precise, and environmentally conscious farming practices essential to meeting the challenges of modern agricultural production (Mahmud et al., 2021).

The magneto-rheological (MR) shock absorber (Abdul Aziz et al., 2022; Ahamed et al., 2018; Cruze et al., 2018; Khedkar et al., 2019; Kumar et al., 2019; Oh & Choi, 2019) is used in vehicle suspension systems, employing magneto-rheological fluids to adjust its stiffness dynamically in real-time. When exposed to a magnetic field, these fluids contain magnetic particles that align with each other, modifying the fluid's properties. This allows continuous adaptation to driving conditions, balancing comfort, and performance. The magneto-rheological shock absorber offers quick response, versatility, comfort, and greater vehicle efficiency. This technology is widely used in the automotive industry to improve ride quality and safety and reduce vibration.

MR fluids continue to be the subject of research and application due to their versatility, controllability, and greater predictability of behavior in different operating modes (Kumar et al., 2019). These attributes are exploited through various methods, including non-linear models, across multiple application areas (Khedkar et al., 2019; Kumar et al., 2019), such as automotive, aerospace, human prosthetics, and other medical and industrial fields. MR is a valuable solution in these applications due to its adaptable properties: viscosity constant, shear rate, controllable flow stress of the MR fluid and magnetic flux density, and the ability to meet specific requirements in different domains (Abdul Aziz et al., 2022; Ahamed et al., 2018; Cruze et al., 2018). Thus, the objective of this work is to mathematically model an orchard tower structure considering tire, motor, and shock absorber, in addition to considering the rheological magnet (MR) to reduce vibration and hysteresis; for our results, we used the phase maps and the FFT (Fast Fourier Transform), and we observed that the application of MR in the structure reduced the vibration frequencies of the non-linear dynamic system obtained.

A vertical dynamic model with four degrees of freedom was developed for the sprayer, which included liquid flow from the tank but did not consider overflow. Increasing frame deflection results in less smooth spraying. By examining the vertical dynamic characteristics at different tank liquid levels, it is confirmed that the impact of liquid splashing on smoothness gradually increases with increasing liquid volume (Lu et al., 2024).

Our manuscript is organized as follows: Section 1 is the mathematical model, where we describe the entire formalism of the equations of motion of the sprayer considered; Section 2 is the methodology applied to obtain the results; Section 3 is the results obtained and their discussions; and finally, the presentation of the conclusions and bibliographical references.

2 MATERIALS AND METHODS

2.1 Discussion of the mathematical model

For the description and discussion of the mathematical model (Cézar, 2014; Sartori, 2008), the diagram in Figure 2 will be considered, which is a description of the mathematical model considering only one of the wheels of the structure represented in the simplified mechanical diagram in Figure 2 (Cunha Jr et al., 2015; Cunha et al., 2017; Sartori et al., 2007).

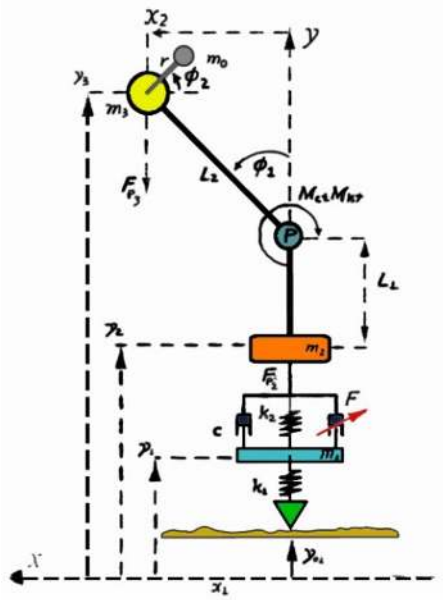

Figure 2: Theoretical diagram of the sprayer analyzed, where x_1 is the horizontal displacement of the trailer, x_2 is the horizontal displacement of the trailer, y_1 is the vertical displacement of the trailer, y_2 is the vertical displacement of the tower, y_3 is the vertical displacement of the tower and trailer assembly, ye_1 is the vertical displacement of the tire, K_1 is the elastic stiffness constant of the tire, k_2 is the elastic stiffness constant of the suspension, K_t is the stiffness of the torsional joint, L_1 is the distance from the CG of the trailer to the "P" junction, L_2 distance from the intersection at point "P" to the tower's center of gravity, m_0 unbalanced mass of the engine, $\mathrm{m}_1$mass of the wheel, m_2 mass of the trailer, m_3 concentrated mass of the fans and engine, ϕ_1 angular displacement of the tower, ϕ_2 angular displacement of the unbalanced engine, r radius of the engine, C damping of the tires, C_T damping of the torsional joint, F damping force, P articulation point of the tower (Cézar, 2014; Sartori, 2008) .

Table 1 shows the structural parameters for mathematical modeling, as shown in Figure 2.

Table 1 Structural parameters considered in the mathematical modeling.

Parameter	Meaning
ϕ_1	Trailer angular displacement
$\dot{\phi}_1$	Angular speed of the trailer
$\ddot{\phi}_1$	Angular acceleration of the trailer
ϕ_2	Angular displacement of the tower
$\dot{\phi}_2$	Angular speed of the tower
$\ddot{\phi}_2$	Angular acceleration of the tower
x_1	Horizontal displacement of the trailer
x_2	Horizontal displacement of the trailer
y_1	Trailer vertical displacement
$\dot{y}_1$	Trailer vertical speed
$\ddot{y}_1$	Trailer vertical acceleration
y_2	Vertical displacement of the tower
y_{e1}	Vertical displacement of the tire
$\dot{y}_{e1}$	Vertical speed of the tire

2.2 Mathematical model

For the mathematical modeling, we consider the kinetic energy (T_T) and the total potential energy (V_T) of the system as:

$$T_T = \frac{1}{2}(m_2 + m_3 + m_0)\dot{y}_2^2 - (m_3 + m_0)L_2\dot{y}_2\dot{\phi}_1 sin\phi_1 + m_3L_2^2\dot{\phi}_1^2 + m_0r^2\dot{\phi}_2^2 +$$

$$m_0\dot{y}_2\dot{\phi}_2 rcos\phi_2 - m_0r\dot{\phi}_1\dot{\phi}_2L_2cos\,(\phi_2 - \phi_1) + \frac{1}{2}m_1\dot{y}_1^2 + \frac{1}{2}m_0L_2^2\dot{\phi}_1^2 \quad (1)$$

$$V_T = \frac{1}{2}K_1(y_1^2 - 2y_1y_{e1} + y_{e1}^2)^2 + \frac{1}{2}K_2(y_1^2 - 2y_1y_2 + y_1^2)^2 + \frac{1}{2}K_T\phi_1^2 \quad (2)$$

The use of the Lagrangian is essential to obtain the equations governing the movement of the system based on Hamilton's principle, providing an efficient way to study and represent intricate dynamic systems. With the Lagrangian, it is possible to obtain the Euler-Lagrange equations, which explain the dynamic behaviour of the system in relation to its generalized coordinates (Silva et al., 2022).

Thus, the total Lagrangian of the system can be expressed as the difference between the total kinetic energy and the total potential energy: $L = T_T - V_T$

$$L = \frac{1}{2}(m_2 + m_3 + m_0)\dot{y}_2^2 - (m_3 + m_0)L_2\dot{y}_2\dot{\phi}_1\,sin\,(\phi_1) + m_3L_2^2\dot{\phi}_1^2 + m_0r^2\dot{\phi}_2^2 + m_0\dot{y}_2\dot{\phi}_2 rcos(\phi_2) - m_0r\dot{\phi}_1$$

$$\dot{\phi}_2L_2\cos(\phi_2 - \phi_1) + \frac{1}{2}m_1\dot{y}_1^2 + \frac{1}{2}m_0L_2^2\dot{\phi}_1^2 - \frac{1}{2}K_1(y_1^2 - 2y_1y_{e1} + y_{e1}^2)^2 - \frac{1}{2}K_2(y_1^2 - 2y_1y_{e1} + y_{e1}^2)^2 - \frac{1}{2}K_T\phi_1^2 \quad (3)$$

Therefore, to determine the equations of motion of the structure defined by Figure (2), we consider the Euler-Lagrange equation defined as:

$$\frac{d}{dt}\left(\frac{\partial L}{\partial \dot{q}_j}\right) - \frac{\partial L}{\partial q_j} = Q_j \quad (4)$$

Since Q_j is the work of all non-conservative forces and is the generalized coordinates (4). q_j $(j = 1, 2, 3, 4)$

However, for the non-conservative forces we consider the suspension damping (F_c), the torsional joint damping (F_{C_T}), the dissipative energy of the Magneto-Rheological damper (MR), therefore:

$$Q_1 = C(\dot{y}_2 - \dot{y}_1) - \delta z \tag{5}$$

$$Q_2 = C(\dot{y}_2 - \dot{y}_1) + \delta z \tag{6}$$

$$Q_3 = -C_T\,\dot{\phi}_1 \tag{7}$$

Where C are tire damping, δ Magneto Rheological damping coupling, and C_T torsional joint damping.

However, Q_4 describe the sprayer motor's non-conservative force, we consider a description of a DC motor. According to (Cveticanin et al., 2018) the interactions between the tower and the DC motor can be simplified by considering the motor's torque, which is expressed as: $M_m = a - b\dot{\phi}_2$. Where a is related to the electrical voltage applied to the DC motor and b is related to the type of motor. Both are defined by $a = \frac{k_m V_a}{R_a}$ e $b = \frac{k_m k_b}{R_a}$, where R_a is the motor's electrical resistance, k_b is the motor's electrical voltage constant, V_a is the input voltage applied to the motor's armature and k_m is the motor's torque constant (Orbolato, 2012). We can therefore write them: Q_4 as:

$$Q_4 = a - b\dot{\phi}_2 \tag{8}$$

The Sprayer (Cézar, 2014; Sartori, 2008) Constant feed with a fan motor is a system consisting of a motor, a fan and a spray mechanism. The motor maintains a constant supply to the sprayer, while the fan, driven by the motor, generates the pressure or flow required to atomize the liquid in the sprayer. The expression mechanism suggests that it may be operating efficiently, which can affect the overall performance of the system.

The modeling of Equation 8 that we used for the motor does not use the ideal voltage, it uses it as a fan to spread the liquid used for spraying.

Thus, by substituting Equations (1)-(3) and Equations (5)-(8) into Equation (4), we will have the set of differential equations that describe the movement of the mechanical system. These equations represent Newton's Laws for the bodies in the system, considering external forces, damping and the stiffness of the springs.

For y_1, the vertical displacement of the tire: sprayer. The expression engine suggests that it may be operating efficiently, which could affect the overall performance of the system.

The modeling of Equation 8 that we used for the motor does not use the ideal voltage, it uses it as a fan to spread the liquid used for spraying (Cunha Jr et al., 2015; Sartori et al., 2007; Silva et al., 2022).

Thus, by substituting Equations (1)-(3) and Equations (5)-(8) into Equation (4), we will have the set of differential equations that describe the movement of the mechanical system. These equations represent Newton's Laws for the bodies in the system, considering the external forces, the damping and the stiffness of the springs.

For y_1, the vertical displacement of the tire:

$$m_1\ddot{y}_1 = -K_1(y_1 - y_{e1}) + K_2(y_2 - y_1) + C(\dot{y}_2 - \dot{y}_1) - \delta z \tag{9}$$

For y_2,the vertical position of the chassis:

$$(m_2 + m_3 + m_0)\ddot{y}_2 - (m_3 + m_0)L_2\ddot{\phi}_1 \sin(\phi_1) + m_0 r\ddot{\phi}_2 cos\phi_2 =$$

$$(m_3 + m_0)L_2\dot{\phi}_1^2 + m_0 r\dot{\phi}_2^2 sin\phi_2 + K_2(y_2 - y_1) + C(\dot{y}_1 - \dot{y}_2) - \delta z \tag{10}$$

For ϕ_1, the angle of inclination of the tower:

$$-(m_3 + m_0)\ddot{y}_2 L_2\phi_1 + 2m_3 L_2^2\ddot{\phi}_1 + m_0 L_2^2\ddot{\phi}_1 - m_0 r L_2\ddot{\phi}_2\, cos\ (\phi_2 - \phi_1)\ = -m_0$$

$$rL_2\dot{\phi}_2\, sin\ (\phi_2 - \phi_1)\left(\dot{\phi}_2 - \dot{\phi}_1\right) - m_0 r L_2\dot{\phi}_2\dot{\phi}_1 sin\,(\phi_2 - \phi_1) - K_T\phi_1 - C_T\dot{\phi}_1 \tag{11}$$

Forϕ_2, angle of inclination of the motor:

$$2m_0 r^2\ddot{\phi}_2 + m_0 r\ddot{y}_2 cos\phi_2 - m_0 r L_2\ddot{\phi}_1 cos(\phi_2 - \phi_1) = -m_0 r L_2\dot{\phi}_1 \sin(\phi_2 - \phi_1)\left(\dot{\phi}_2 - \dot{\phi}_1\right) + m_0 r L_2\dot{\phi}_1\dot{\phi}_2$$

$$sin\ (\phi_2 - \phi_1)\ + (\hat{a} - \hat{b}\dot{\phi}_2) \tag{12}$$

The Bouc-Wen model is extremely versatile and can exhibit a wide variety of hysteretic behavior. It contains viscous damper components, a spring, and a hysteretic component (Ribeiro et al., 2022). To evaluate the performance of MR dampers in vibration control applications, many researchers adopt the Bouc-Wen model (Ambhore et al., 2013; Parlak et al., 2022).

To describe the behavior of Magneto Rheological (MR), we consider the following Equation (13):

$$\dot{z} = -\gamma|\dot{y}_2 - \dot{y}_1|z|z^{(n-1)} - \beta(\dot{y}_2 - \dot{y}_1)|z|^n + \nwarrow (\dot{y}_2 - \dot{y}_1) \tag{13}$$

Where γ, β, n and $\nwarrow$are parameters relating to the shape and size of the hysteresis curve formed by the MR, which are related to the MR's damping capacity and stiffness.

The equations provided describe a non-linear dynamic system for the movement of our structure. So, we can rewrite the system of equations considering $\dot{x}_1 = x_2, \dot{x}_2 = x_3, \dot{x}_3 = x_4, \dot{x}_4 = x_5, \dot{x}_5 = x_6, \dot{x}_6 = x_7, \dot{x}_7 = x_8, \dot{x}_8 = x_9$. Next:

$$\dot{x}_1 = x_2$$

$$\dot{x}_2 = -\frac{K_1}{m_1}(x_1 - y_{e1}) + \frac{K_2}{m_1}(x_3 - x_1) + \frac{C}{m_1}(x_4 - x_2) - \delta x_9$$

$$\dot{x}_3 = x_4$$

$$\dot{x}_4 = \frac{1}{m_2+m_3+m_0}[(m_3 + m_0)L_2 x_6^2 cos\ (x_5)\ sin\ (x_5)\ + (m_0 r x_8^2 sin\ (x_7)\ + K_2(x_3 - x_1) + C(x_2 - x_4) - \delta x_9\ ]$$

$$\dot{x}_5 = x_6$$

$$\dot{x}_6 = -\frac{(m_3+m_0)L_2}{2m_3L_2}x_4 x_5 cos\ (x_5)\ sin(x_5) + \frac{(2m_3L_2^2)(2m_3L_2^2)}{m_0}x_6 - \frac{m_0 r L_2}{2m_3L_2} - cos\ (x_7 - x_5) + \frac{m_0 L_2^2}{2m_3}x_6 - \frac{m_0 r L_2}{2m_3 L_2}\ x_8\ sin\ (x_7 - x_5)\ + \frac{K_T}{m_3 L_2^2}x_5 - \frac{C_T}{m_3 L_2^2}x_6$$

$$\dot{x}_7 = x_8$$

$$\dot{x}_8 = \frac{1}{2m_0 r}(x_8)\ - m_0 r L_2 cos\ (x_7 - x_5)x_6 sin(x_8))\frac{m_0 r L_2 x_6 x_8 sin\ (x_7 - x_5)}{2m_0 r^2} + \frac{a^2 - b^2 x_8}{2m_0 r^2}$$

$$\dot{x}_9 = -\gamma|x_4 - x_2|x_9|x_9|^{(n-1)} - \beta(x_4 - x_2)|x_9|^n + \nwarrow (x_4 - x_2) \tag{14}$$

For better clarification, Figures 3 and 4 show the description of the structural parameters and their interferences in the movement of the sprayer.

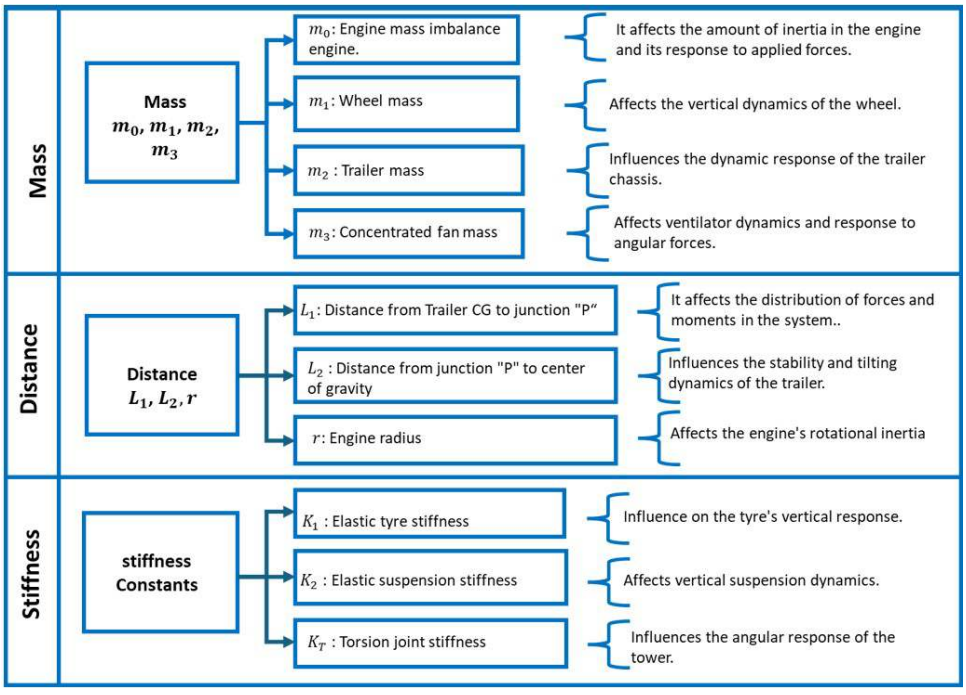

Figure 3: Structural parameters and their influence on sprayer movement.

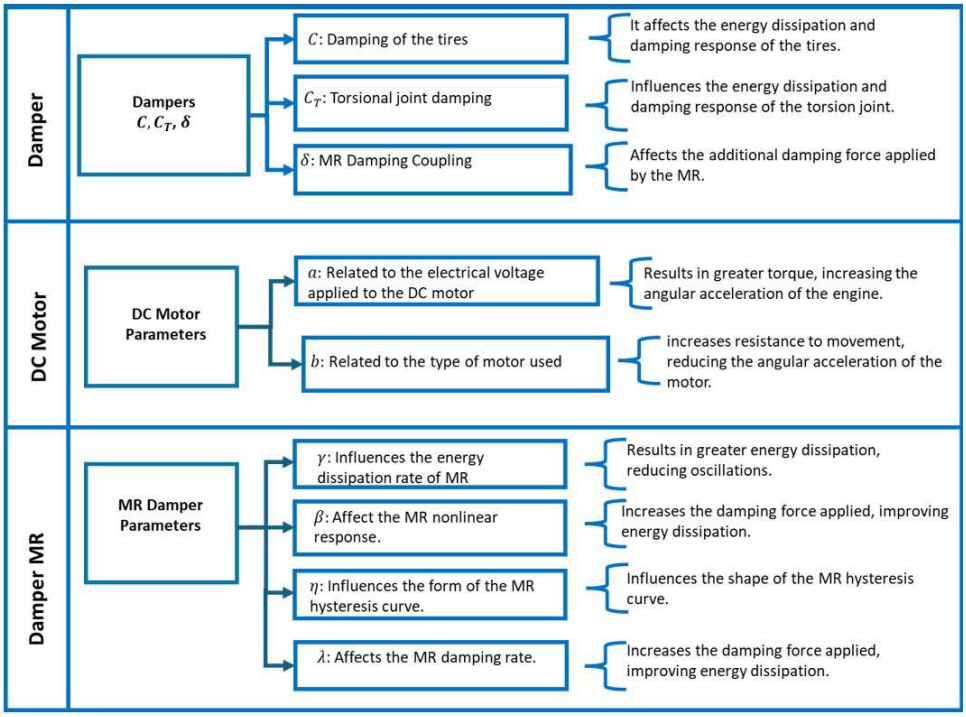

Figure 4: Parameters of the non-conservative forces and their influence on the sprayer's movement.

3 NUMERICAL ANALYSIS AND RESULTS

To analyze the mathematical model proposed by Equations (14), a numerical analysis was carried out to determine the behavior of the time series and phase maps. The time series describes the behavior of the displacements described by equations (14) over time, and the phase maps illustrate the behavior of the trajectories of these time series. To obtain these results, we used the 4th-order Runge and Kutta (RK) method (Lin et al., 2010) with an integration step of h=0.001 and a total computer simulation time of 10^6[s] so that we could respect the convergence of the method. The (RK) method is widely used for integrating non-linear differential equations such as those described in our manuscript's mathematical model (Silva et al., 2022).

With these results, the fast Fourier transform (FFT) was used for frequency analysis. FFT is in line with (Harčarik et al., 2012). It is a powerful tool that allows us to express any periodic signal or function as a combination of more straightforward trigonometric functions, such as sines and cosines. The great advantage of the Fourier method lies in its ability to break down a complex function into more basic and understandable components. In mechanical engineering, the Fast Fourier Transform (FFT) is often used to convert digital signals from the time domain to the frequency domain. This approach is precious for identifying the modal vibration parameters in mechanical systems. If noise is generated during system vibration, it is possible to record it in a digital wave file. This data can then be processed for further analysis and understanding of the system's behavior.

Table (2) describes the parameters used for the computer simulations of the mathematical model proposed by Equations (9-13).

Where, K_T and C_T represents the spring and damping parameters of the rotational system. This system of first-order differential equations is now in the form of a state space, where x is the state vector and u is the input vector.

Figure 5 shows how the manuscript was created, starting with the description of the parameters and ending with the analysis and simulation of the mathematical model.

The parameters described in table 2 were used for the simulation. In this way, we analyzed two cases: the first is without applying MR to the structure ($\delta = 0$). We can see that there is a frequency peak in the FFT as shown in Figure (6) (d), the largest peak represents the dominant frequency of the system which is 0.1445 Hz and three smaller frequency peaks 0.1747 Hz, 0.1125 Hz and 0.02603 Hz. Figures (6) (a) show the phase space behavior of the trailer structure in which the parameters are described in Table 2, i.e. without damping. And Figures (6)(b) and (c) show the time series of x_3 e x_4, respectively.

Table 2 Parameters used for the computer simulations of the mathematical model. Adapted from

Description	Parameter	Value	Unit
Constant elastic stiffness of the tire	K_1	46500	N/m
Constant elastic stiffness of the suspension	K_2	3610	N/m
Torsional joint stiffness	K_T	5000	Nm/rad
Damping of the tires	C	784	Ns/m
Torsional joint damping	C_T	1000	Nms/rad
Engine mass imbalance	m_0	2.5	Kg
Wheel mass	m_1	600	Kg
Trailer mass	m_2	3250	Kg
Engine mass	m	2.0	Kg
Concentrated fan mass	m_3	800	800 Kg
Magneto-Rheological Damping Coupling	δ	300000	N/m
Engine radius	r	0,6	m
Distance from Trailer CG to junction “P”	L_1	0,2	m
Distance from junction “P” to center of gravity	L_2	2,4	m
Related to the electrical voltage applied to the DC motor	a	3.0	V
Related to the type of motor used	b	1.0	-
Parameter dependent on damper characteristics	γ	800	$1/m^2$
Constant varies damper characteristics	n	2	$1/m^2$
Constant depending on damper characteristics	β	1000000	$1/m^2$
Constant depending on damper characteristics	$\searrow$	1.0	-

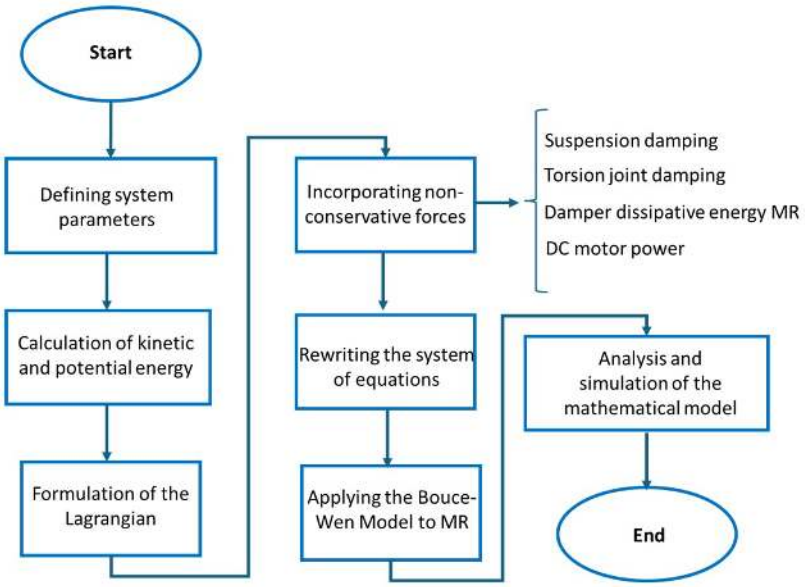

Figure 5: Shows how the work was carried out.

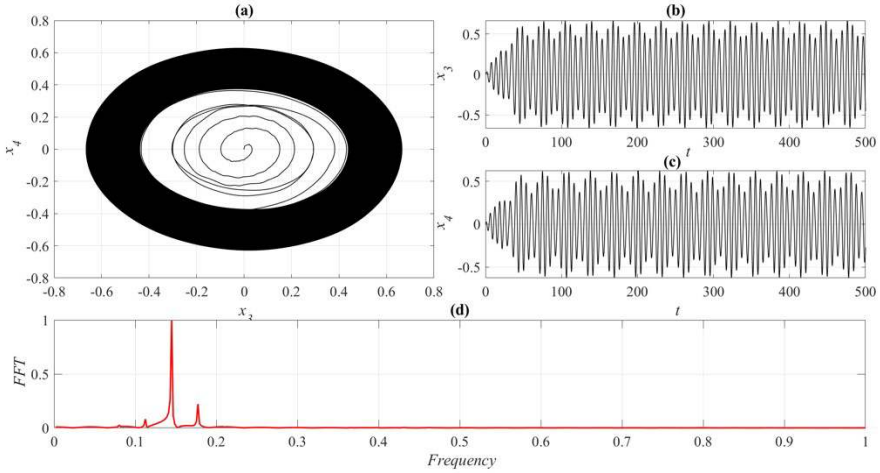

Figure 6: (a) phase map without MR, (b) and (c) time series without MR and (d) FFT without MR.

The second case is with the application of MR to the structure ($\delta \neq 0$), the value considered is described in Table 2. In this case, there was a reduction in the vibrations caused during the sprayer operation process. Figure (7) (a)-(c) shows the behavior of the phase map and the time series of the trailer's displacement during the spraying process, and Figure (7)(d) represents the FFT with the application of MR. We can see in Figure (7)(d) that there are no more minor peak vibrations, as observed in Figure (7)(d). This shows that the application of MR reduces the intensity of the lower frequency peaks and leaves only the dominant frequency of the system (the peak with the highest intensity).

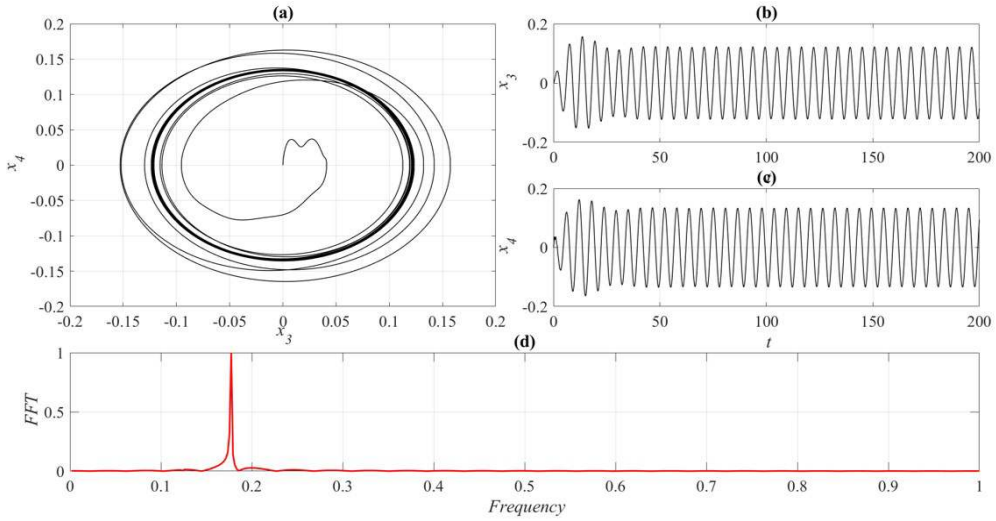

Figure 7: (a) phase map with MR, (b) and (c) time series with MR and (d) FFT with MR.

Considering Figure 8, the amplitude without the application of MR has a maximum of 0.6651 Hz and with the application of MR there was a reduction to 0.1575 Hz. In other words, there was a 23.68% reduction in the trailer's vibration amplitude.

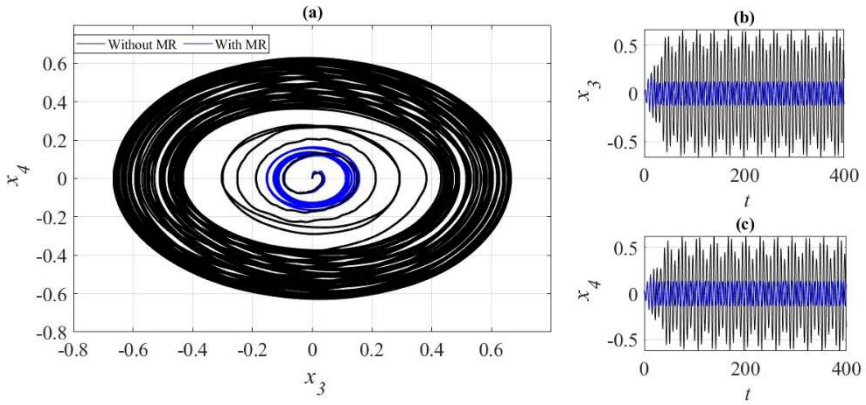

Figure 8: Comparison between the amplitudes of the time series, black line without MR, blue line with MR (a), (b) and (c).

According to Sartori (2008), equipment like tower sprayers with reservoirs that can be empty, partially filled, or fully filled can reach speeds of up to 20 Km/h on terrain characterized by low amplitude and high frequency. However, during the spraying process, the tank starts full and gradually empties, causing the sprayer to operate at speeds between 2 and 6 Km/h, depending on the terrain in the application region.

According to the technical specifications from Jacto S/A (2024b), the tank capacity can reach up to 4,000 liters for applying agricultural pesticides in orchards, while the application trailer weighs 2,350 kg. However, for our numerical analyses, we considered a tank filled with 900 liters of agricultural pesticides, totaling 3,250 kg.

Our numerical results revealed the benefits of applying MR during the spraying process, showing a reduction in the vibration of the arm attached to the sprayer. Although MR resulted in reduced vibrations, as shown in the FFT graphs, it primarily reduced the amplitude of the system's displacement in these results. Therefore, to validate the numerical findings, we plan to experimentally investigate the proposed mathematical model.

4 CONCLUSIONS

The mathematical model, combined with the numerical analysis, demonstrated that applying MR to the tower sprayer's structure resulted in a 23.68% reduction in the amplitude of the trailer's vibrations.

By comparing two scenarios in the numerical analysis of the mathematical model, with and without the use of MR, we determined that the presence of MR contributed to a significant reduction in vibration amplitudes. The FFT analysis revealed that the application of MR suppressed the lower frequency peaks, maintaining only the dominant frequency of the system. The smaller peaks identified in the scenario without MR were effectively reduced, promoting more stable and controlled behavior during the spraying process.

Thus, the use of MR in the tower sprayer's structure not only demonstrated effectiveness in reducing vibrations, but also, together with the proposed mathematical model, showed the practical feasibility and effectiveness of implementing MR fluids as a strategy for reducing vibrations in agricultural systems, significantly improving the operation and stability of similar equipment. Therefore, to validate the numerical results, we intend to investigate the proposed mathematical model experimentally in future manuscript.

Author's Contributions: Conceptualization, R.N. Silva and M. Ribeiro; Methodology, R.N. Silva, J. Balthazar and M. Ribeiro; Investigation, R.N. Silva, J. Balthazar and M. Ribeiro; Redaction – R.N. Silva, J. Balthazar and M. Ribeiro; review and editing, R.N. Silva and J. Balthazar; Software, R.N. Silva and M. Ribeiro; Preview, R.N. Silva, A. Tusset.

Editor: Marcílio Alves

References

Abdul Aziz, M., Muhtasim, S., & Ahammed, R. (2022). State-of-the-art recent developments of large magnetorheological (MR) dampers: a review. In Korea Australia Rheology Journal (Vol. 34, Número 2). Korean Society of Rheology, Australian Society of Rheology. https://doi.org/10.1007/s13367-022-00021-2

Ahamed, R., Choi, S. B., & Ferdaus, M. M. (2018). A state of art on magneto-rheological materials and their potential applications. Journal of Intelligent Material Systems and Structures, 29(10), 2051–2095. https://doi.org/10.1177/1045389X18754350

Ambhore, N., Hivarale, S., & Pangavhane, D. R. (2013). A Study of Bouc-Wen Model of Magnetorheological Fluid Damper for Vibration Control. International Journal of Engineering Research and Technology, 2(2), 1–6. www.ijert.org

Americo Cunha Jr, Jorge Luis Palacios Felix, & José Manoel Balthazar. (2015). On the nonlinear dynamics of an inverted double pendulum over a vehicle suspension subject to random excitations. Proceedings of the 23rd ABCM International Congress of Mechanical Engineering, 2007. https://doi.org/10.20906/cps/cob-2015-1694

Arvidsson, V., Holmström, J., & Lyytinen, K. (2014). Information systems use as strategy practice: A multi-dimensional view of strategic information system implementation and use. Journal of Strategic Information Systems, 23(1), 45–61. https://doi.org/10.1016/j.jsis.2014.01.004

Cézar, É. S. (2014). Metodologia de sistema de controle para uma suspensão veicular com magneto reologico (mr) para um pulverizador do tipo torre (Número 12030204039). Universidade Federal do Pampa.

Cruze, D., Hemalatha, G., Jebadurai, S. V. S., Sarala, L., Tensing, D., & Christy, S. S. J. E. (2018). A Review on the Magnetorheological Fluid, Damper and Its Applications for Seismic Mitigation. Civil Engineering Journal, 4(12), 3058. https://doi.org/10.28991/cej-03091220

Cunha, A., Palacios Felix, J. L., & Balthazar, J. M. (2017). Quantification of parametric uncertainties induced by irregular soil loading in orchard tower sprayer nonlinear dynamics. Journal of Sound and Vibration, 408, 252–269. https://doi.org/10.1016/j.jsv.2017.07.023

Cveticanin, L., Zukovic, M., & Balthazar, J. M. (2018). Dynamics of Mechanical Systems with Non-Ideal Excitation. In Springer (p. 227). https://doi.org/10.1007/978-3-319-54169-3

Dekeyser, D., Duga, A. T., Verboven, P., Endalew, A. M., Hendrickx, N., & Nuyttens, D. (2013). Assessment of orchard sprayers using laboratory experiments and computational fluid dynamics modelling. Biosystems Engineering, 114(2), 157–169. https://doi.org/10.1016/j.biosystemseng.2012.11.013

Garcerá, C. et al. (2017). Spray pesticide applications in mediterranean citrus orchards: Canopy deposition and off-target losses. Science of the Total Environment, 599, 1344–1362.

Grella, M., Marucco, P., Manzone, M., Gallart, M., & Balsari, P. (2017). Effect of sprayer settings on spray drift during pesticide application in poplar plantations (*Populus* spp.). The Science of the Total Environment, 578, 427–439. https://doi.org/10.1016/j.scitotenv.2016.10.205

Harčarik, T., Bocko, J., & Masláková, K. (2012). Frequency analysis of acoustic signal using the Fast Fourier Transformation in MATLAB. Procedia Engineering, 48(December 2012), 199–204. https://doi.org/10.1016/j.proeng.2012.09.505

Hołownicki, R., Doruchowski, G., Świechowski, W., Godyń, A., & Konopacki, P. J. (2017). Variable air assistance system for orchard sprayers; concept, design and preliminary testing. Biosystems Engineering, 163(November), 134–149. https://doi.org/10.1016/j.biosystemseng.2017.09.004

Jacto S/A. (2024a). ARBUS 4000 MULTISPRAYER. https://s3.amazonaws .com/1 -jacto.com. br/files/product_file_file_ pt_BR_1714324303494_Jacto-fl-Arbus_ 4000_ Multisprayer-2024-digital.pdf, access: 16/07/2024

Jacto S/A. (2024b). Máquinas Agrícolas Jacto S.A. https://jacto.com/brasil/products/pulverizador-autonomo/arbus-4000-jav.

Kasner, E. J., Fenske, R. A., Hoheisel, G. A., Galvin, K., Blanco, M. N., Seto, E. Y. W., & Yost, M. G. (2020). Spray Drift from Three Airblast Sprayer Technologies in a Modern Orchard Work Environment. Annals of Work Exposures and Health, 64(1), 25–37. https://doi.org/10.1093/annweh/wxz080

Khedkar, Y. M., Bhat, S., & Adarsha, H. (2019). A review of magnetorheological fluid damper technology and its applications. International Review of Mechanical Engineering, 13(4), 256–264. https://doi.org/10.15866/ireme.v13i4.17224

Kira, O., Dubowski, Y., & Linker, R. (2018). In-situ open path FTIR measurements of the vertical profile of spray drift from air-assisted sprayers. Biosystems Engineering, 169, 32–41. https://doi.org/10.1016/j.biosystemseng.2018.01.010

Kumar, J. S., Paul, P. S., Raghunathan, G., & Alex, D. G. (2019). A review of challenges and solutions in the preparation and use of magnetorheological fluids. International Journal of Mechanical and Materials Engineering, 14(1). https://doi.org/10.1186/s40712-019-0109-2

Li, T., Qi, P., Wang, Z., Xu, S., Huang, Z., Han, L., & He, X. (2022). Evaluation of the Effects of Airflow Distribution Patterns on Deposit Coverage and Spray Penetration in Multi-Unit. Agronomy, 12, 944.

Lin, R., Wang, C., Liu, F., & Xu, Y. (2010). A new numerical method of nonlinear equations by four order Runge-Kutta method. IEEM2010 - IEEE International Conference on Industrial Engineering and Engineering Management, 1295–1299. https://doi.org/10.1109/IEEM.2010.5674394

Lu, L., Zhang, J., Cui, C., Chen, J., Chen, Y., Jing, H., Zhang, S., Adilet, S., Hu, C., & Cao, J. (2024). Influences of the tank liquid lateral sloshing and mass time-varying on high clearance self-propelled sprayer ride comfort. International Journal of Agricultural and Biological Engineering, 17(1), 12-22. https://doi.org/10.25165/j.ijabe.20241701.7798

Ma, C., Li, G., & Peng, Q. (2021). Design and Test of a Jet Remote Control Spraying Machine for Orchards. AgriEngineering, 3(4), 797–814. https://doi.org/10.3390/agriengineering3040050

Mahmud, M. S., Zahid, A., He, L., & Martin, P. (2021). Opportunities and possibilities of developing an advanced precision spraying system for tree fruits. In Sensors (Vol. 21, Número 9, p. 3262). https://doi.org/10.3390/s21093262

McCoy, M. L., Hoheisel, G. A., & Moyer, M. M. (2023). Survey of Pacific Northwest Grapegrowers on Their Use, Choice, and Understanding of Vineyard Canopy Sprayers. American Journal of Enology and Viticulture, 74(2). https://doi.org/10.5344/ajev.2023.23053

Miranda-Fuentes, A., Rodríguez-Lizana, A., Gil, E., Agüera-Vega, J., & Gil-Ribes, J. A. (2015). Influence of liquid-volume and airflow rates on spray application quality and homogeneity in super-intensive olive tree canopies. Science of the Total Environment, 537, 250–259. https://doi.org/10.1016/j.scitotenv.2015.08.012

Oh, J.-S., & Choi, S.-B. (2019). A Review on the Development of Dampers Utilizing Smart Magnetorheological Fluids. Current Smart Materials, 4(1), 15–21. https://doi.org/10.2174/2405465804666190408153926

Orbolato, L. M. T. (2012). Análise do comportamento sismico das partes internas de um equipamento de proteção ambiental. Escola Politécnica da Universidade de São Paulo (in portuguese).

Ozkan, E. (2022). Best Practices for Effective Spraying in Orchards and Vineyards. Ohio State University Extension, FABE-539, 4–6.

Parlak, Z., Soylemez, M. E., & Sahin, I. (2022). A New Methodology to Describe Non-Linear Characterization Depending on Temperature of a Semi-Active Absorber Based on Bouc-Wen Model. Gazi University Journal of Science, 35(4), 1624–1638. https://doi.org/10.35378/gujs.930412

Patil, S. S. et al. (2023). Review on Automatic Variable-Rate Spraying Systems Based on Orchard Canopy Characterization. Informatics and Automation, 22(1), 57–86. https://doi.org/10.15622/ia.22.1.3

Ribeiro, M. A., Balthazar, J. M., Lenz, W. B., Felix, J. L. P., Litak, G., & Tusset, A. M. (2022). Oscillator Including Non-Ideal Motor Excitation. Axioms, 667. https://doi.org/10.3390/axioms11120667

Sartori, J. S., Balthazar, J. M., & Pontes, B. R. D. J. (2007). Modelo dinâmico de um pulverizador torre baseado em um pêndulo invertido. XXXVI Congresso Brasileiro de Engenharia Agrícola (in portuguese).

Sartori, S. J. (2008). Modelagem matemática e análise dinâmica da torre de um pulverizador de pomares. Faculdade de Engenharia da Universidade Estadual Paulista “Julio de Mesquita Filho” (in portuguese).

Silva, R. N., Felix, J. L. P., Balthazar, J. M., Tusset, A. M., Ribeiro, M. A., Lenz, W. B., & Cunha, A. (2022). On a Vehicular Suspension for a Non-ideal and Nonlinear Orchard Tower Sprayer Through an Inverted Pendulum Using Reologic Magneto (MR) BT - Nonlinear Vibrations Excited by Limited Power Sources (J. M. Balthazar (org.); p. 151–173). Springer International Publishing. https://doi.org/10.1007/978-3-030-96603-4_10

van Zyl, J. G., Sieverding, E. G., Viljoen, D. J., & Fourie, P. H. (2014). Evaluation of two organosilicone adjuvants at reduced foliar spray volumes in South African citrus orchards of different canopy densities. Crop Protection, 64, 198–206. https://doi.org/10.1016/j.cropro.2014.06.024

Xun, L., Garcia-Ruiz, F., Fabregas, F. X., & Gil, E. (2022). Pesticide dose based on canopy characteristics in apple trees: Reducing environmental risk by reducing the amount of pesticide while maintaining pest and disease control efficacy. Science of the Total Environment, 826(February), 154204. https://doi.org/10.1016/j.scitotenv.2022.154204